

## **PETCT Imaging of Unstable Carotid Plaque with Ga-68 labelled Somatostatin Receptor Ligand**

Ming Young Simon Wan<sup>1</sup>, Raymond Endozo<sup>1</sup>, Sofia Michopoulou<sup>1</sup>, Robert Shortman<sup>1</sup>,  
Manuel Rodriguez-Justo<sup>2</sup>, Leon Menezes<sup>1</sup>, Syed Yusuf<sup>3</sup>, Toby Richards<sup>4</sup>, Damian Wild<sup>5</sup>,  
Beatrice Waser<sup>6</sup>, Jean Claude Reubi<sup>6</sup>, Ashley Groves<sup>1</sup>

### **Authors' Affiliation**

1. Institute of Nuclear Medicine, 2. Department of Histopathology, 4. Department of Vascular Surgery, University College London, London, United Kingdom

3. Department of Vascular Surgery, Brighton and Sussex University Hospitals, Sussex, United Kingdom

5. Division of Nuclear Medicine, University of Basel Hospital, Basel, Switzerland

6. Cell Biology and Experimental Cancer Research, Institute of Pathology, University of Berne, Berne, Switzerland

**Specific contribution** - see cover letter

### **Author for correspondence**

Ming Young Simon Wan, Institute of Nuclear Medicine, T5, University College Hospital, United Kingdom, NW2 1BU. [mwan@nhs.net](mailto:mwan@nhs.net) 44-2034470565. Fax44-2034470598.

**First Authors (not in training)**

MYS Wan, [mwan@nhs.net](mailto:mwan@nhs.net)

Institute of Nuclear Medicine, T5, University College Hospital, United Kingdom, NW2 1BU.

Tel 44-2034470565. Fax 44-2034470598.

**Disclosure**

This work was partially undertaken at UCLH/UCL who received a proportion of funding from the Department of Health's NIHR Biomedical Research Centre's funding scheme.

All authors have control of all data and information submitted.

**Running Title** Ga68-DOTATATE PETCT vulnerable plaques

**Word count** 4998

## **ABSTRACT**

Ga68 labelled somatostatin receptor ligand PET imaging has recently been shown in preclinical and early human studies to have a potential role in the evaluation of vulnerable arterial plaques. We prospectively evaluated carotid plaque Ga68-DOTATATE uptake in patients with recent carotid events, assessed inter- and intra- observer variability of such measurements, and explored the mechanism of any plaque DOTATATE activity with immunohistochemistry in resected specimens.

### **Methods:**

20 consecutively consenting patients with recent symptomatic carotid events (transient ischaemic attack, stroke or amaurosis fugax), due for carotid endarterectomy were prospectively recruited. Ga68-DOTATATE PET/CT of the neck was performed prior to surgery. Ga68-DOTATATE uptake was measured by drawing regions of interest (ROI) along the carotid plaques and contralateral plaques/carotid arteries by experienced radionuclide radiologist and radiographer. Two PET quantification methods with inter- and Intra-observer variability were assessed. Resected carotid plaques were retrieved for sst-2 immunohistochemical stain.

### **Results:**

Median time delay between research PET and surgery was 2days. SUV and TBR values for the symptomatic plaques and the asymptomatic contralateral carotid arteries/plaques show no significant difference ( $n=19$ ,  $p$ -value  $>0.10$ ), regardless of quantification method. Intraclass correlation coefficient was  $>0.8$  in all measures of carotid artery/plaque uptake

(SUV) and  $>0.6$  in almost all measures of target-to-background ratio (TBR). None of the excised plaques were shown to contain cells (macrophages, lymphocytes, vessel-associated cells) expressing sst2 on their cell membrane.

### **Conclusion:**

Ga68 DOTATATE activity on PET in recently symptomatic carotid plaques is not significantly different to contralateral carotids/plaques. Any activity seen on PET is not shown to be from specific sst2 receptor-mediated uptake *in-vitro*. It is therefore unlikely that sst2 PET/CT imaging will have a role in the detection and characterization of symptomatic carotid plaques.

### **Key words**

Somatostatin

PETCT

DOTATATE

Carotid

Vulnerable plaques

## INTRODUCTION

Atherosclerosis is a leading cause of mortality and morbidity. There is the concept that while atherosclerotic plaques may contribute to symptoms by luminal stenosis, it is the disruption of unstable plaques, which leads to catastrophic events, including stroke and myocardial infarction. Termed 'vulnerable plaques', these unstable plaques are believed to have characteristic features such as inflammatory cells infiltration, lipid core and fibrous cap (1,2).

Measuring the degree of luminal stenosis was the mainstay of assessment and directed management decisions until recently (3-5). Recognition of its limitation has driven the use of biomarkers such as fractional flow reserve in coronary disease and exploration of functional imaging to non-invasively identify vulnerable plaques (6,7).

Radionuclide imaging has the advantageous capability of directly probing molecular mechanisms *in-vivo* using radioactive tracers (8). In particular, assessment of plaque inflammation using F18-FDG (flurodeoxyglucose) PETCT (positron emission tomography/computed tomography) has been extensively studied. Since early validation studies (9,10), plaque F18-FDG uptake has been associated with cardiovascular risk factors and circulating inflammatory markers (11,12). It can predict future cardiovascular risk in asymptomatic individuals (13) and early stroke recurrence (14). Further studies have shown its potential in evaluating treatment response with statins (15). Moreover, FDG PET has become the primary endpoint in some drug trials assessing the drugs' anti-inflammatory effect (16,17). Despite the success, extension of its use to coronary vessels is limited by

variably high background myocardial FDG activity. This has fueled motivation to explore alternative PET tracers (18).

Inflammatory cells involved in the pathophysiology of atherosclerosis (19) may express somatostatin receptors (20,21). It is also known that vessels can express somatostatin receptors under certain conditions (22,23). Recently, two preclinical murine studies have demonstrated potential of somatostatin receptor PET in atherosclerosis imaging (24,25). Retrospective human studies with these tracers have also shown promise (26-29). In this study, we prospectively explored the use of a clinically established PET tracer, Gallium68-[1,4,7,10-tetraazacyclododecane-N,N',N'',N9'''-tetraacetic acid]-D-Phe<sup>1</sup>,Tyr<sup>3</sup>-octreotate (Ga68-DOTATATE), a somatostatin receptor ligand, in patients whom are believed to have vulnerable carotid plaques, based on recent symptomatic events. We hypothesized that Ga68-DOTATATE uptake is measurably higher on PETCT in vulnerable carotid plaques, compared to contralateral carotid arteries/plaques. We assessed two quantification methods, adapted from previous carotid PET tracer-histological validation studies. Inter-observer and intra-observer agreement were tested. As a secondary imaging endpoint, we studied the relationship of PET uptake with plaque composition on CT angiogram (CTA). This latter had been shown to correlate well with histology (30). Finally, we studied the subsequently excised carotid endarterectomy samples with emphasis on somatostatin subtype-2 (sst2) immunohistochemistry.

## **MATERIALS AND METHODS**

## **Patients**

Institutional review board approved this study. All subjects signed a written informed consent. 20 consecutive consenting patients were recruited. Inclusion criteria were patients planned for carotid endarterectomy for recent symptomatic events (stroke, transient ischaemic attack or amaurosis fugax). They were identified from well-established regional hyperacute stroke unit and transient ischaemic attack clinics. As per local routine, the diagnosis was confirmed by specialist stroke physicians. Other potential mechanisms of these symptoms were reasonably excluded. These patients had >70% carotid stenosis confirmed by two concordant imaging modalities of CTA down to aortic arch, magnetic resonance angiogram or duplex ultrasound. These were interpreted by local experts using the European Carotid Surgery Trial and North American Symptomatic Carotid Endarterectomy grading for carotid stenosis (4,5). The patients' management was fully discussed at multidisciplinary board meetings attended by specialist stroke physicians, vascular surgeons and neuroradiologists. Here, the etiology of the presumed carotid events was scrutinized. Consensus was made in this forum, that vulnerable carotid plaque was the likely culprit, and that the patient was deemed at high risk for further events. Plan for carotid endarterectomy was agreed here. Only cases clearly attributed to the carotid and high risk were considered for this study. Exclusion criteria were age <45, pregnancy and lactation and inability to consent.

## **Imaging**

All patients underwent Ga68-DOTATATE PET/CT prior to surgery. An additional CTA was performed at the same time for superior coregistration of Ga68-DOTATATE uptake and carotid plaque, unless precluded by renal failure.

Synthesis and labelling of Ga68-DOTATATE has been published previously (31). Our radiopharmacy has an average radiochemical purity of 99% (range 98-99.9%) for this tracer. Patients were given Ga68-DOTATATE injection (mean activity received 157MBq) with uptake time of 60 minutes. All PETCT were performed on the same scanner (DiscoveryVCT, GE Healthcare). A single bed acquisition was performed to image the carotid arteries. CT parameters were: 120kVp, mA modulation 30-300mAs, noise index 20, pitch 1.375, rotation time 800msec, pixel size 0.98mm and 2.5mm slice thickness. This was followed by an emission scan with 3D acquisition over 4 minutes, iterative reconstruction (OSEM 20 subset 2 iterations), 3.27mm slice thickness and 5.5mm pixel size. Attenuation correction was performed with the non-contrast CT. CTA was performed as published previously (32).

### **PET Analysis**

There is no established method for quantification of Ga68-DOTATATE PET in this context. We drew on previous published carotid PET tracer-histological validation studies for the two methods used (10,32,33). Images were analyzed using Xeleris (GE Healthcare). Carotid plaques were identified using CTA as part of this study, or in a few patients with renal failure, from imaging acquired at the time of their acute presentation day(s) prior to the



research PETCT. The location of the carotid plaques on PET was identified by either fusing the PET and CTA images or by reviewing the imaging side-by-side.

Plaque uptake was measured by drawing ROI around the carotid arteries at every slice, where (i) plaques were visible, and (ii) around the carotid bifurcation (up to 2cm superior and 1cm inferior to the bifurcation). If no clear plaque was seen on a given slice (as was often the case on the asymptomatic side, on eventual unblinding of reader), ROI was placed around the carotid arteries at the same axial slices as any contralateral carotid plaque to allow comparison. In each ROI, the mean and maximum standardized uptake values (SUV) were calculated (Bq/mL). Average blood pool activity for each patient was derived from averaging at least three different ROI in venous structures, usually at the most distended segment of the jugular vein.

Measurements from the ROI were computed in two different ways to reflect two different quantification methods of Ga68-DOTATATE uptake:

Volume plaque method: mean and maximum pixel activities for the ROI in all the slices in a plaque/vessel defined above were averaged to give 'SUVmean' & 'SUVmax' of the plaques. These were also corrected for blood pool activity, by division by the average blood pool activity, to derive target-to-background measurements: 'TBRmean' & 'TBRmax'.

Most intense pixel/ROI method: the single pixel with the most intense signal and the ROI with the most intense averaged SUV value in a plaque/vessel were selected. These

were designated 'maxSUVmax' and 'maxSUVmean'. These were corrected for blood pool activity as above to derive 'maxTBRmax' & 'maxTBRmean'.

### **Inter- and Intra-Observer Variability**

To assess intra-observer variability, PET analysis was performed twice by reader 1, a PET accredited radiologist with interest in cardiovascular imaging, with an 8 week period in between. Inter-observer variability was assessed by a further analysis by reader 2, a superintendent radiographer with prior experience in similar carotid PET quantification. The two readers co-read several pilot studies (not included in this study) to establish a standard protocol for analysis. All images were analyzed with the readers blinded to the side of symptoms.

### **Plaque Composition Analysis**

Carotid plaques on the symptomatic side were manually segmented slice-by-slice on the CTA using ADW (GE Healthcare) workstation. The lumen was segmented out manually. Plaque composition in individual pixel was assigned based on density (Hounsfield unit of 20-60 were assigned as lipid, 60-130 as fibrous, and >130 as calcification) (32,34). Plaque components were expressed as percentage of overall plaque volume.

### **Histological Analysis**

All patients proceeded to have carotid endarterectomy using an eversion endarterectomy technique, by one of three dedicated surgeons on next available list. Plaques

were immediately fixed in 10% buffered formalin and decalcified following standard protocol at University College London Hospitals. Specimens were transversely sectioned at 5-mm intervals, embedded face up in paraffin, and cut at 3-4- $\mu$ m thickness. Haematoxylin and eosin sections were obtained and the plaque was typed according to American Heart Association criteria (2). Pan-macrophage marker immunostaining (CD68) was performed as previously described (32).

Sst2 immunohistochemistry was performed at the University of Berne, where there is established expertise in somatostatin immunohistochemistry, as previously published using sst2 antibody UMB1 (35). Tissues known to express sst2 (neuroendocrine tumours, germinal centres and peritumoral vessels) were used as positive controls (21,23). Sst<sub>2</sub> immunohistochemistry has been selected because Ga-DOTATATE is known to be highly selective for sst2 labeling (36). There is no reason to believe that it would label another sst subtype in these tissues. Samples were sent from London to Berne in batches, with 10 randomly selected samples initially, followed by batch of 3 specifically selected for their highest Ga68-DOTATATE signals on PETCT.

### **Statistical Analysis**

Statistical tests were performed using SPSS version 21. Statistical significance was assigned for  $p < 0.05$ . Normality of measurements was tested with Shapiro-Wilk test and visual inspection. Two-tailed paired sample *t*-test was used to compare uptake between the symptomatic and asymptomatic sides. Intra-class correlation coefficient was used to assess intra-observer variability (1-way random effects model with absolute agreement) and inter-

observer variability (2-way mixed effects model with absolute agreement) (37). Spearman rank correlation was used to assess relationship of PET signal with CT plaque components, and Kruskal-Wallis test for the relationship of immunohistochemistry with PET signal.

## **RESULTS**

Patient demographics, risk factors and medications are presented on Table 1. All excised symptomatic plaques were considered advanced by American Heart Association histological criteria (type V or VI). Detailed histological features are presented on Supplemental Table 1.

### **Imaging Findings**

One patient had focal intense uptake in the asymptomatic carotid bifurcation, corresponding to a previously un-diagnosed carotid body tumour. This patient was excluded. There was no statistically significant difference between symptomatic carotid plaques and asymptomatic carotid plaques/arteries (Fig. 1) in any of the SUV and TBR measurements (Table 2; Fig. 2; Supplemental Fig. 1 and 2).

All values for SUV measurements are  $>0.9$ , with narrow confidence intervals, indicating excellent agreement. Values for TBR measurements are almost exclusively  $>0.6$ , indicating substantial agreement. (Supplemental Table 2).

There was no statistically significant correlation between any SUV and TBR parameters with the CT plaque composition parameters (Supplemental Table 3).

## Immunohistochemistry Findings

Variable CD68 staining was observed in the excised plaques, at values comparable to previous carotid plaque imaging-histological investigations (32) (Supplemental Table 1). There was no statistically significant relationship of CD68 with any SUV and TBR parameters (Supplemental Table 4).

None of the tissues were shown to contain cells expressing sst2 on their cell membrane (Figure 3), a major criteria for G-protein coupled receptor specificity (28). Moreover, no non-specific labeling, i.e. no cytoplasmic staining of the cells, was detected in the analyzed tissues.

## DISCUSSION

In this prospective study of Ga68-DOTATATE PETCT with histological validation of human vulnerable carotid plaques, we addressed the pertinent question of whether sst2 expressing cells (believed to be macrophages) are present in these plaques, in sufficient density for detection with Ga68-DOTATATE PET/CT *in vivo*. We demonstrated that measurement of vascular uptake with Ga68-DOTATATE PETCT in carotid plaques was feasible, using two different PET quantification methods, with both showing substantial to excellent agreements. However, we did not find significantly higher Ga68-DOTATATE activity in vulnerable carotid plaques, compared to the contralateral carotids/plaques. Sst2-immunohistochemistry was chosen for its established, direct relevance to Ga68-DOTATATE-sst2 binding at the cell surface (in contrast to mRNA/PCR or macrophage cluster of differentiation markers). Despite confirmation of the presence of CD68+

macrophages, none of the excised plaques examined showed cells expressing sst2 on their cell membrane, indicating that there is no molecular basis for an sst2 receptor mediated uptake of somatostatin tracer *in vitro* in acute human plaques. Our findings would not support the use of Ga68-DOTATATE in the detection and characterization of vulnerable plaques in human.

### **Rationale for Study of Ga68-DOTATATE in Atherosclerosis**

Monocytes and macrophages were the first inflammatory cells to be associated with atherosclerosis. They are believed to play important roles in its pathogenesis, contributing to necrotic core formation and fibrous cap thinning in advanced atherosclerosis, features thought to confer 'vulnerability' (19,38). It is known that human macrophages express sst2 on their cell surface in cell culture experiments (20,39). Ga68-DOTATATE, a specific sst2 receptor agonist, therefore was thought to have the potential to be a surrogate marker of inflammation to study plaque biology. This has been recently validated in two preclinical murine experiments (apolipoprotein -/- mice model) at a tissue level (24,25).

### **Human Studies with Somatostatin Receptor PET**

Four recent studies examined the potential role of these in atherosclerosis, retrospectively in patients with neuroendocrine tumours.

One found significant correlation between TBR with calcific plaque burden and prior vascular events (26). Another found that TBR at areas of focal vessel uptake are

higher in patients with more cardiovascular risk factors (27). A further study found increase Ga68-DOTATATE uptake in coronary plaques compared to normal coronary segments (28). The last compared Ga68-DOTATOC and Cu64-DOTATATE (29), in correlating vessel uptake against cardiovascular risk factors. Cu64-DOTATATE demonstrated higher uptake compared to Ga68-DOTATOC, with positive correlation with Framingham scores only with Cu64-DOTATATE, but not with Ga68-DOTATOC.

To our knowledge, there has been one prospective study specifically looking at vulnerable plaque (40). This examined 10 patients with stroke or transient ischaemic attack with Cu64-DOTATATE. The authors found higher uptake in the symptomatic plaque compared to the contralateral carotid vessel. Significant but weak association was demonstrated between uptake on PET and CD163 and CD68 gene expression in endarterectomy samples on univariate analysis, with CD163 remaining significant on multivariate analysis. CD163 is believed to be a marker of M2 (alternatively activated) macrophages, found in haemorrhagic zones of plaques and possibly has an anti-inflammatory function.

### **Interpretation in Context of Published Literature**

The preclinical promise has not translated into a positive result in our study. A plausible explanation may be species-specific variability of sst subtype expression. For instance, human chronic atherosclerotic popliteal arteries were found to show consistently higher sst1 expression compared to sst2 or sst4, which differed from the predominant sst2&3 expression in rat vessels (41). In addition, although macrophage activation is a

feature of inflammation in atherosclerosis development, there are conflicting results in the published preclinical human cell experiments as to whether sst2 expression on macrophages signifies their activation (20,25,39). Our validation on human vulnerable plaques is more directly relevant to clinical practice. Our results would suggest lack of significant sst2 expression in macrophages present in recently symptomatic plaques.

Our study also adds to current knowledge in that unlike our study, the retrospective studies above did not allow study of causation, or molecular mechanism of any observed tracer activity, to the clinical parameters observed. These were also performed in patients with chronic plaques only. It should be noted that plaque FDG uptake has been shown to evolve over the chronic course of disease (42). It is likely that Ga68-DOTATATE uptake would behave similarly. One of the retrospective studies (27) showed poor co-localization of FDG and Ga68-DOTATATE signal in vessels. FDG activity in plaques is established as a surrogate marker of plaque inflammation, validated against macrophage cell surface marker (CD68) in a number of studies (9,10). Poor co-localization of the Ga68-DOTATATE and FDG signal therefore raises serious question about the meaning of any observed DOTATATE (& FDG) signal. The only published prospective study on Cu64-DOTATATE did not examine sst2 expression in the resected tissue (40).

Taken together, it is likely that there are complex relationships between stage of plaque evolution (chronic versus acute), macrophage density and activity, sst subtype expression, FDG and somatostatin receptor PET signal. Macrophage subtype/activation in vulnerable human atherosclerosis plaques have been studied recently *in vitro*, generally



showing higher expression of pro-inflammatory M1 macrophages compared to M2 macrophages, which may be anti-atherogenic (43-45). How this interacts with Ga68-DOTATATE signal needs to be further explored.

## Limitations

Our sample size is small and this raises possibility of false negative study. However our negative imaging findings were supported by robust histological examination of *ex-vivo* samples, performed in a laboratory with long held expertise in sst receptor studies. The antibodies used was the current gold standard of sst2 immunostaining which had been extensively evaluated previously (35,46). Moreover, our sample size was comparable to other similar carotid imaging-histological validation investigations (10,18,33). There is heterogeneity of time between carotid event, research PET and endarterectomy in our patients. This reflects the logistical challenge surrounding patient recruitment, tracer, scanner and operating theatre availability. However, the ranges of delay are comparable with similar studies. We performed single time point imaging at 60 minutes only. Bulk of the retrospective data on vascular DOTATATE PET uptake had similar uptake time. In addition, an 'early' scan ([median] 85 minutes) with Cu64-DOTATATE has already been shown to be preferred, compared to delayed acquisition (40).

Ga68 has less optimal imaging characteristics compared to F18 or Cu64. Ga68 DOTATATE may be less sensitive to weak differences in uptake compared to equivalent Cu64 labelled tracers (29). Higher image noise is reflected by poorer inter- and intra-

observer agreement of TBR measurements, in face of excellent agreement in SUV measurements – while the arterial plaques provide a clear target for directing ROI placement, ROI for blood pool may be more operator dependent; image noise and variation in blood pool measurements therefore manifest as poorer TBR agreement. Increasing acquisition time beyond 4 minutes may counter this, but at the expense of risk of detrimental patient movement and misregistration.

Spillover & partial volume effect from adjacent structures is a concern, with major salivary glands and thyroid shown to have SUVmax of 2.3-4.2(31), higher than vascular activity observed. There may also be increased activity in adjacent nodes. ROI were drawn carefully to minimize these.

## **CONCLUSION**

We demonstrated feasibility of Ga68-DOTATATE measurement of carotid plaques on PETCT. However, we found no significant difference in Ga68DOTATATE activity in symptomatic carotid plaques compared to the asymptomatic side. This finding was supported by compelling lack of sst2 expression on excised plaques. Our findings indicate no molecular basis for an sst2 receptor mediated uptake of the somatostatin tracer *in vitro* and would not support use of Ga68-DOTATATE PET in assessment of acute vulnerable human plaques.

## **ACKNOWLEDGEMENTS**

This work was partially undertaken at UCLH/UCL who received a proportion of funding from the Department of Health's NIHR Biomedical Research Centre's funding scheme.

## REFERENCES

1. Shah PK. Mechanisms of plaque vulnerability and rupture. *J Am Coll Cardiol.* 2003;41:S15-S22.
2. Stary HC, Chandler AB, Dinsmore RE, et al. A Definition of Advanced Types of Atherosclerotic Lesions and a Histological Classification of Atherosclerosis A Report From the Committee on Vascular Lesions of the Council on Arteriosclerosis, American Heart Association. *Arterioscler Thromb Vasc Biol.* 1995;15:1512-1531.
3. Optimal medical therapy with or without PCI for stable coronary disease. *N Engl J Med.* 2007;356.
4. Randomised trial of endarterectomy for recently symptomatic carotid stenosis: final results of the MRC European Carotid Surgery Trial (ECST). *The Lancet.* 1998;351:1379-1387.
5. Beneficial effect of carotid endarterectomy in symptomatic patients with high-grade carotid stenosis. *N Engl J Med.* 1991;325:445-453.
6. Nicolaidis AN, Kakkos SK, Kyriacou E, et al. Asymptomatic internal carotid artery stenosis and cerebrovascular risk stratification. *J Vasc Surg.* 2010;52:1486-1496 e1481-1485.
7. De Bruyne B, Pijls NH, Kalesan B, et al. Fractional flow reserve-guided PCI versus medical therapy in stable coronary disease. *N Engl J Med.* 2012;367:991-1001.
8. Evans NR, Tarkin JM, Chowdhury MM, Warburton EA, Rudd JH. PET Imaging of Atherosclerotic Disease: Advancing Plaque Assessment from Anatomy to Pathophysiology. *Curr Atheroscler Rep.* 2016;18:30.
9. Rudd JHF. Imaging Atherosclerotic Plaque Inflammation With [18F]-Fluorodeoxyglucose Positron Emission Tomography. *Circulation.* 2002;105:2708-2711.
10. Tawakol A, Migrino RQ, Bashian GG, et al. In vivo 18F-fluorodeoxyglucose positron emission tomography imaging provides a noninvasive measure of carotid plaque inflammation in patients. *J Am Coll Cardiol.* 2006;48:1818-1824.
11. Yoo HJ, Kim S, Park MS, et al. Vascular inflammation stratified by C-reactive protein and low-density lipoprotein cholesterol levels: analysis with 18F-FDG PET. *J Nucl Med.* 2011;52:10-17.
12. Noh TS, Moon SH, Cho YS, et al. Relation of carotid artery 18F-FDG uptake to C-reactive protein and Framingham risk score in a large cohort of asymptomatic adults. *J Nucl Med.* 2013;54:2070-2076.
13. Figueroa AL, Abdelbaky A, Truong QA, et al. Measurement of arterial activity on routine FDG PET/CT images improves prediction of risk of future CV events. *JACC Cardiovasc Imaging.* 2013;6:1250-1259.
14. Marnane M, Merwick A, Sheehan OC, et al. Carotid plaque inflammation on 18F-fluorodeoxyglucose positron emission tomography predicts early stroke recurrence. *Ann Neurol.* 2012;71:709-718.

15. Tahara N, Kai H, Ishibashi M, et al. Simvastatin attenuates plaque inflammation: evaluation by fluorodeoxyglucose positron emission tomography. *J Am Coll Cardiol*. 2006;48:1825-1831.
16. Comparison of clopidogrel versus ticagrelor therapy for atherosclerotic plaque inflammation. *ClinicalTrials.gov*. Accessed September 28, 2016
17. The effect(s) of sevelamer carbonate (renvela) on atherosclerotic plaque inflammation judged by FDG-PET scan. *ClinicalTrials.gov*. Accessed September 28, 2016
18. Joshi NV, Vesey AT, Williams MC, et al. 18F-fluoride positron emission tomography for identification of ruptured and high-risk coronary atherosclerotic plaques: a prospective clinical trial. *The Lancet*. 2014;383:705-713.
19. Moore Kathryn J, Tabas I. Macrophages in the Pathogenesis of Atherosclerosis. *Cell*. 2011;145:341-355.
20. Armani C, Catalani E, Balbarini A, Bagnoli P, Cervia D. Expression, pharmacology, and functional role of somatostatin receptor subtypes 1 and 2 in human macrophages. *J Leukoc Biol*. 2007;81:845-855.
21. Reubi JC, Horisberger U, Kappeler A, Laissue JA. Localization of Receptors for Vasoactive Intestinal Peptide, Somatostatin and Substance P in Distinct Compartments of Human Lymphoid Organs. *Blood*. 1998;92:191-197.
22. Reubi JC, Mazzucchelli L, Laissue JA. Intestinal vessels express a high density of somatostatin receptors in human inflammatory bowel disease. *Gastroenterology*. 1994;106:951-959.
23. Reubi JC, Mazzucchelli L, Hennig I, Laissue JA. Local upregulation of neuropeptide receptors in host blood vessels around human colorectal cancers. *Gastroenterology*. 1996;110:1719-1726.
24. Rinne P, Hellberg S, Kiugel M, et al. Comparison of Somatostatin Receptor 2-Targeting PET Tracers in the Detection of Mouse Atherosclerotic Plaques. *Mol Imaging Biol*. 2016;18:99-108.
25. Li X, Bauer W, Kreissl MC, et al. Specific somatostatin receptor II expression in arterial plaque: (68)Ga-DOTATATE autoradiographic, immunohistochemical and flow cytometric studies in apoE-deficient mice. *Atherosclerosis*. 2013;230:33-39.
26. Rominger A, Saam T, Vogl E, et al. In vivo imaging of macrophage activity in the coronary arteries using 68Ga-DOTATATE PET/CT: correlation with coronary calcium burden and risk factors. *J Nucl Med*. 2010;51:193-197.
27. Li X, Samnick S, Lapa C, et al. 68Ga-DOTATATE PET/CT for the detection of inflammation of large arteries: correlation with 18F-FDG, calcium burden and risk factors. *EJNMMI Res*. 2012;2:52.

28. Mojtahedi A, Alavi A, Thamake S, et al. Assessment of vulnerable atherosclerotic and fibrotic plaques in coronary arteries using 68Ga-DOTATATE PET/CT. *Am J Nucl Med Mol Imaging*. 2015;5:65-71.
29. Malmberg C, Ripa RS, Johnbeck CB, et al. 64Cu-DOTATATE for Noninvasive Assessment of Atherosclerosis in Large Arteries and Its Correlation with Risk Factors: Head-to-Head Comparison with 68Ga-DOTATOC in 60 Patients. *Journal of Nuclear Medicine*. 2015;56:1895-1900.
30. de Weert TT, Ouhlous M, Meijering E, et al. In vivo characterization and quantification of atherosclerotic carotid plaque components with multidetector computed tomography and histopathological correlation. *Arterioscler Thromb Vasc Biol*. 2006;26:2366-2372.
31. Shastry M, Kayani I, Wild D, et al. Distribution pattern of 68Ga-DOTATATE in disease-free patients. *Nucl Med Commun*. 2010;31:1025-1032.
32. Menezes LJ, Kotze CW, Agu O, et al. Investigating vulnerable atheroma using combined (18)F-FDG PET/CT angiography of carotid plaque with immunohistochemical validation. *J Nucl Med*. 2011;52:1698-1703.
33. Beer AJ, Pelisek J, Heider P, et al. PET/CT imaging of integrin alphavbeta3 expression in human carotid atherosclerosis. *JACC Cardiovasc Imaging*. 2014;7:178-187.
34. Homburg PJ, Rozie S, van Gils MJ, et al. Association Between Carotid Artery Plaque Ulceration and Plaque Composition Evaluated With Multidetector CT Angiography. *Stroke*. 2011;42:367-372.
35. Korner M, Waser B, Schonbrunn A, Perren A, Reubi JC. Somatostatin Receptor Subtype 2A Immunohistochemistry Using a New Monoclonal Antibody Selects Tumors Suitable for In Vivo Somatostatin Receptor Targeting. *Am J Surg Pathol*. 2012;36:242-252.
36. Reubi JC, Schar JC, Waser B, et al. Affinity profiles for human somatostatin receptor subtypes SST1-SST5 of somatostatin radiotracers selected for scintigraphic and radiotherapeutic use. *Eur J Nucl Med Mol Imaging*. 2000;27:273-282.
37. McGraw KO, Wong SP. Forming Inferences about Some Intraclass Correlation Coefficients. *Psychological Methods*. 1996;1:30-46.
38. Woollard KJ, Geissmann F. Monocytes in atherosclerosis: subsets and functions. *Nat Rev Cardiol*. 2010;7:77-86.
39. Dalm VASH, van Hagen PM, Van Koetsveld PM, et al. Expression of somatostatin, cortistatin, and somatostatin receptors in human monocytes, macrophages, and dendritic cells. *Am J Physiol Endocrinol Metab*. 2003;285:E344-E353.
40. Pedersen SF, Sandholt BV, Keller SH, et al. 64Cu-DOTATATE PET/MRI for Detection of Activated Macrophages in Carotid Atherosclerotic Plaques Studies in Patients Undergoing Endarterectomy. *Arterioscler Thromb Vasc Biol*. 2015;35:1696-1703.

- 41.** Curtis SB, Hewitt J, Yakubovitz S, Anzarut A, Hisang YN, Buchan AMJ. Somatostatin receptor subtype expression and function in human vascular tissue. *Am J Physiol Heart Circ Physiol.* 2000;278:H1815-H1822.
- 42.** Menezes LJ, Kayani I, Ben-Haim S, Hutton B, Eil PJ, Groves AM. What is the natural history of 18F-FDG uptake in arterial atheroma on PET/CT? Implications for imaging the vulnerable plaque. *Atherosclerosis.* 2010;211:136-140.
- 43.** Shaikh S, Brittenden J, Lahiri R, Brown PA, Thies F, Wilson HM. Macrophage subtypes in symptomatic carotid artery and femoral artery plaques. *Eur J Vasc Endovasc Surg.* 2012;44:491-497.
- 44.** Cho KY, Miyoshi H, Kuroda S, et al. The phenotype of infiltrating macrophages influences arteriosclerotic plaque vulnerability in the carotid artery. *J Stroke Cerebrovasc Dis.* 2013;22:910-918.
- 45.** Medbury HJ, Williams H, Fletcher JP. Clinical significance of macrophage phenotypes in cardiovascular disease. *Clinical and Translational Medicine.* 2014;3:42.
- 46.** Fisher T, Doll C, Jacobs S, Kolodziej A, Stumm R, Schulz S. Reassessment of sst2 somatostatin receptor expression in human normal and neoplastic tissues using the novel rabbit monoclonal antibody UMB-1. *J Clin Endocrinol Metab.* 2008;93:4519-4524.

## FIGURES

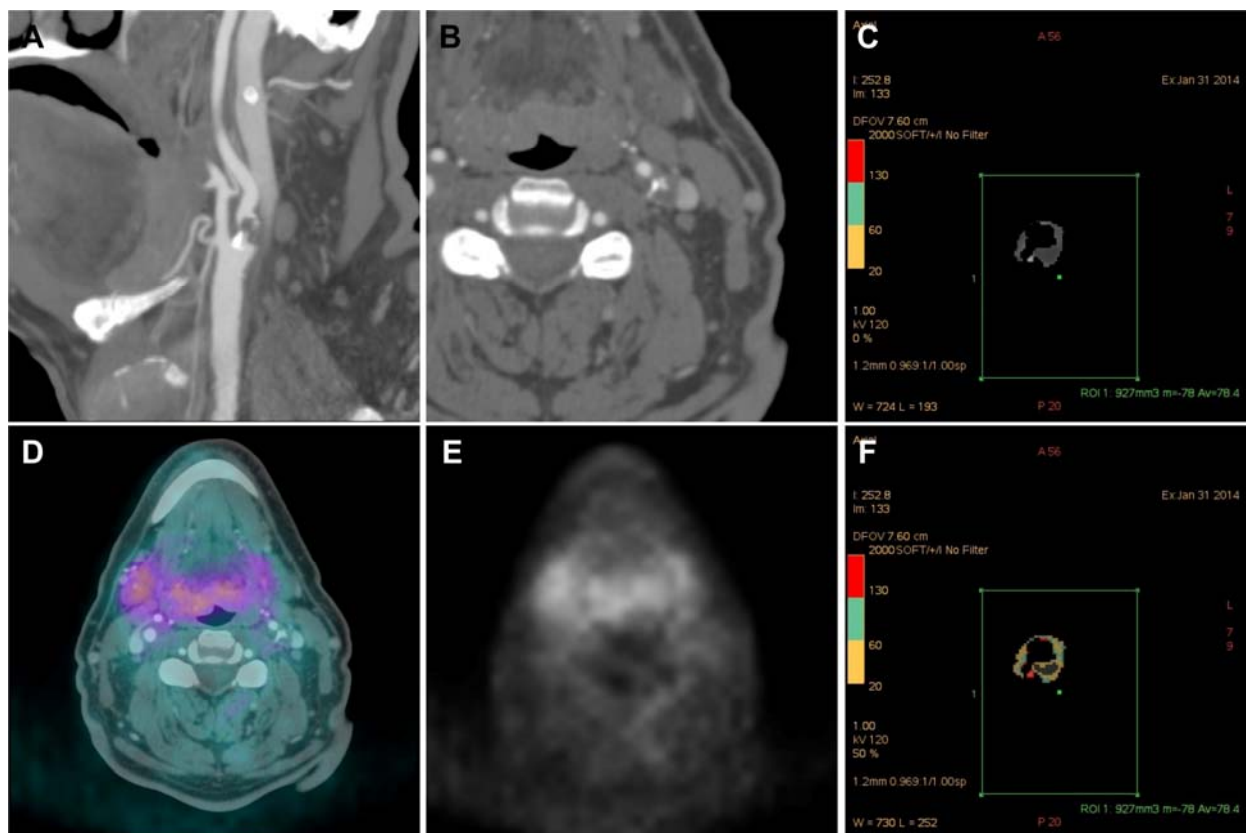


Figure 1. Images from a 68-year-old male with multiple recent left amaurosis fugax. A,B: CTA shows severe stenosis of the left internal carotid artery extending from the bifurcation; D,E: fused and PET image at this level; C,F: segmented plaque on CTA from a different level, with colour coded scale showing plaque compositions.



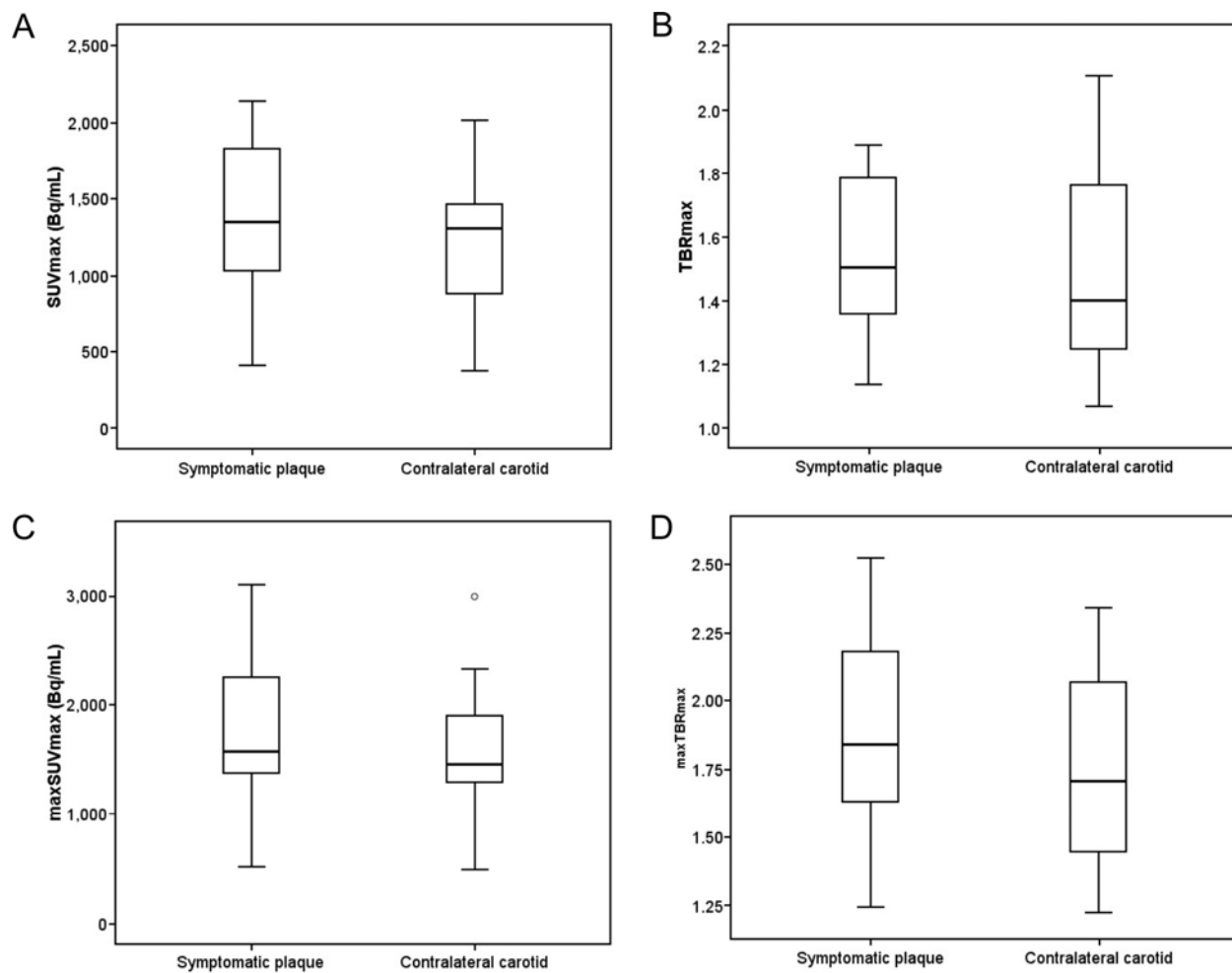


Figure 2. Box whisker plots showing no significant difference in SUV and TBR parameters between the symptomatic and the asymptomatic side.

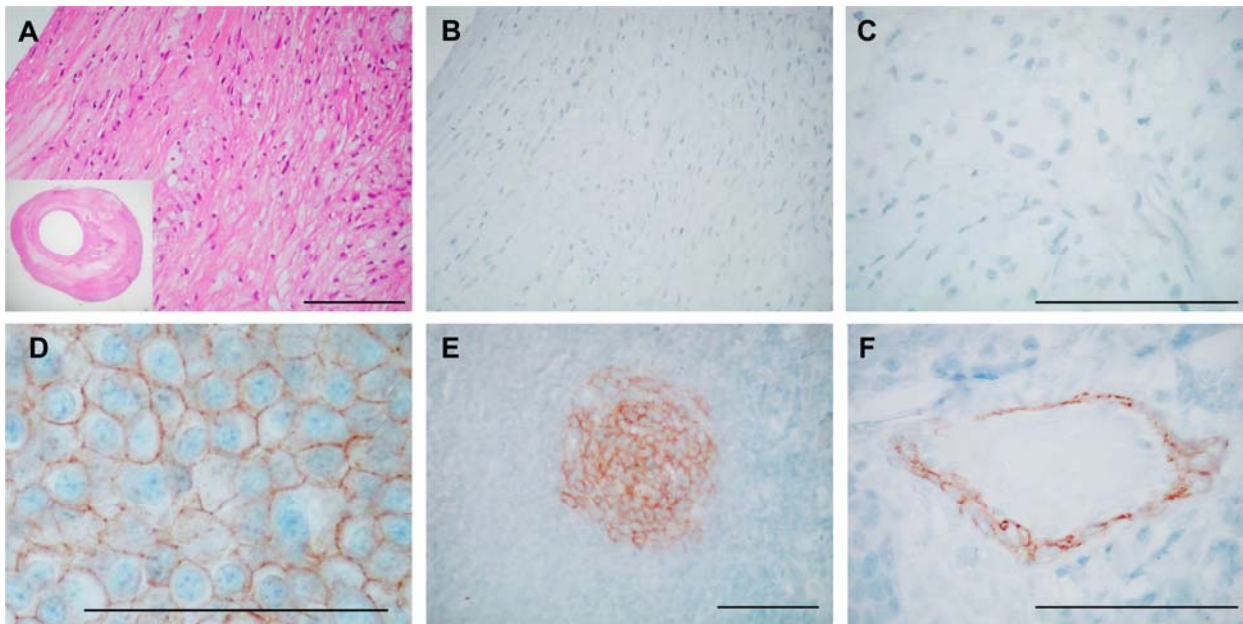


Figure 3: Sst2 immunohistochemistry showing absence of sst2 in a representative carotid plaque. A: Hematoxylin-eosin staining of a representative part of the plaque (insert shows the whole plaque). B: Sst2 immunohistochemistry of adjacent section showing absence of sst2. C: Sst2 immunohistochemistry at higher magnification. D-F: Positive sst2 immunohistochemistry in 3 different reference control tissues: D: neuroendocrine tumor cells. E: Lymphocytes in gut germinal centre. F: Endothelial cells in peritumoral vessel. Bars = 0.1 mm.

**TABLES**

Table 1.

Characteristics	Value
Age(years: mean+/-standard deviation)	78.5+/-9.5
Sex(male:female)	12:8
Time between symptom to PETCT(days:median;range)	6.5;2-27
Time between PETCT to endarterectomy(days:median;range)	2;0-6
<b>Diagnosis</b>	
Stroke	40%
Transient ischaemic attack	30%
Amaurosis fugax	30%
<b>Cardiovascular Risk Factors</b>	
Hypertension	85%
Smoker	45%
Previous transient ischaemic attack/stroke	35%
Previous ischaemic heart disease	40%
Diabetes	30%
Atrial fibrillation	15%
Hypercholesterolaemia	65%
<b>Medications at presentation</b>	
Aspirin	40%
Clopidogrel	10%
Warfarin	10%
Statins	55%
Ezetimibe	15%

Table 2. SUV and TBR between the symptomatic and the asymptomatic sides.

Volume plaque method				
	SUVmax	SUVmean	TBRmax	TBRmean
<i>p</i> -value	0.223	0.784	0.507	0.707
Most intense pixel/ROI method				
	maxSUVmax	maxSUVmean	maxTBRmax	maxTBRmean
<i>p</i> -value	0.098	0.897	0.248	0.810

**SUPPLEMENTAL DATA**

Supplemental Table 1. Histological type (American Heart Association criteria) and features of excised plaques &amp; CD68 result

Patient Number	Plaque type	Lipid core	Thrombus	Intraplaque haemorrhage	Ulceration	CD68
1	Vb	Yes	No	No	No	>15%
2	VI	Yes	No	No	Yes	>15%
3	VI	Yes	No	No	Yes	5-15%
4	Vb	Yes	No	No	No	5-15%
5	Vb	Yes	No	No	No	>15%
6	Va	No	No	No	No	<5%
7	Va	No	No	No	No	5-15%
8	VI	Yes	No	Yes	Yes	>15%
9	Va	Yes	No	No	No	>15%
10	Va	Yes	No	No	No	>15%
11	VI	Yes	No	No	Yes	>15%
12	Vb	No	No	No	No	5-15%
13	VI	No	No	No	Yes	5-15%
14	Vb	No	No	No	No	<5%
15	Vb	No	No	No	No	5-15%
16	Vb	Yes	No	No	No	5-15%
17	Vc	No	No	No	No	5-15%
18	VI	Yes	No	Yes	No	>15%
19	VI	Yes	No	No	Yes	<5%
20	Vb	Yes	No	No	No	>15

Supplemental Table 2. Intraclass correlation coefficient

Volume plaque method		Intra-observer	Inter-observer*
Endarterectomy	SUVmax	0.98(0.94-0.99)	0.97(0.91-0.99)
	SUVmean	0.98(0.96-0.99)	0.98(0.95-0.99)
	TBRmax	0.71(0.41-0.87)	0.61(0.25-0.83)
	TBRmean	0.75(0.48-0.89)	0.63(0.25-0.84)
Contralateral	SUVmax	0.98(0.96-0.99)	0.97(0.90-0.99)
	SUVmean	0.99(0.98-1.00)	0.98(0.97-1.00)
	TBRmax	0.80(0.57-0.92)	0.63(0.26-0.84)
	TBRmean	0.83(0.61-0.93)	0.72(0.38-0.89)
Most intense pixel/ROI value method		Intra-observer	Inter-observer*
Endarterectomy	maxSUVmax	0.94(0.85-0.98)	0.96(0.88-0.98)
	maxSUVmean	0.95(0.89-0.98)	0.93(0.84-0.97)
	maxTBRmax	0.70(0.40-0.87)	0.61(0.24-0.83)
	maxTBRmean	0.82(0.61-0.93)	0.48(0.03-0.76)
Contralateral	maxSUVmax	0.99(0.97-1.00)	0.95(0.84-0.98)
	maxSUVmean	0.99(0.97-1.00)	0.97(0.93-0.99)
	maxTBRmax	0.79(0.55-0.92)	0.77(0.46-0.91)
	maxTBRmean	0.84(0.64-0.94)	0.73(0.40-0.89)

\*excludes 1 outlier

Supplemental Table 3. CT plaque composition analysis & correlation with Ga68DOTATATE uptake parameters.

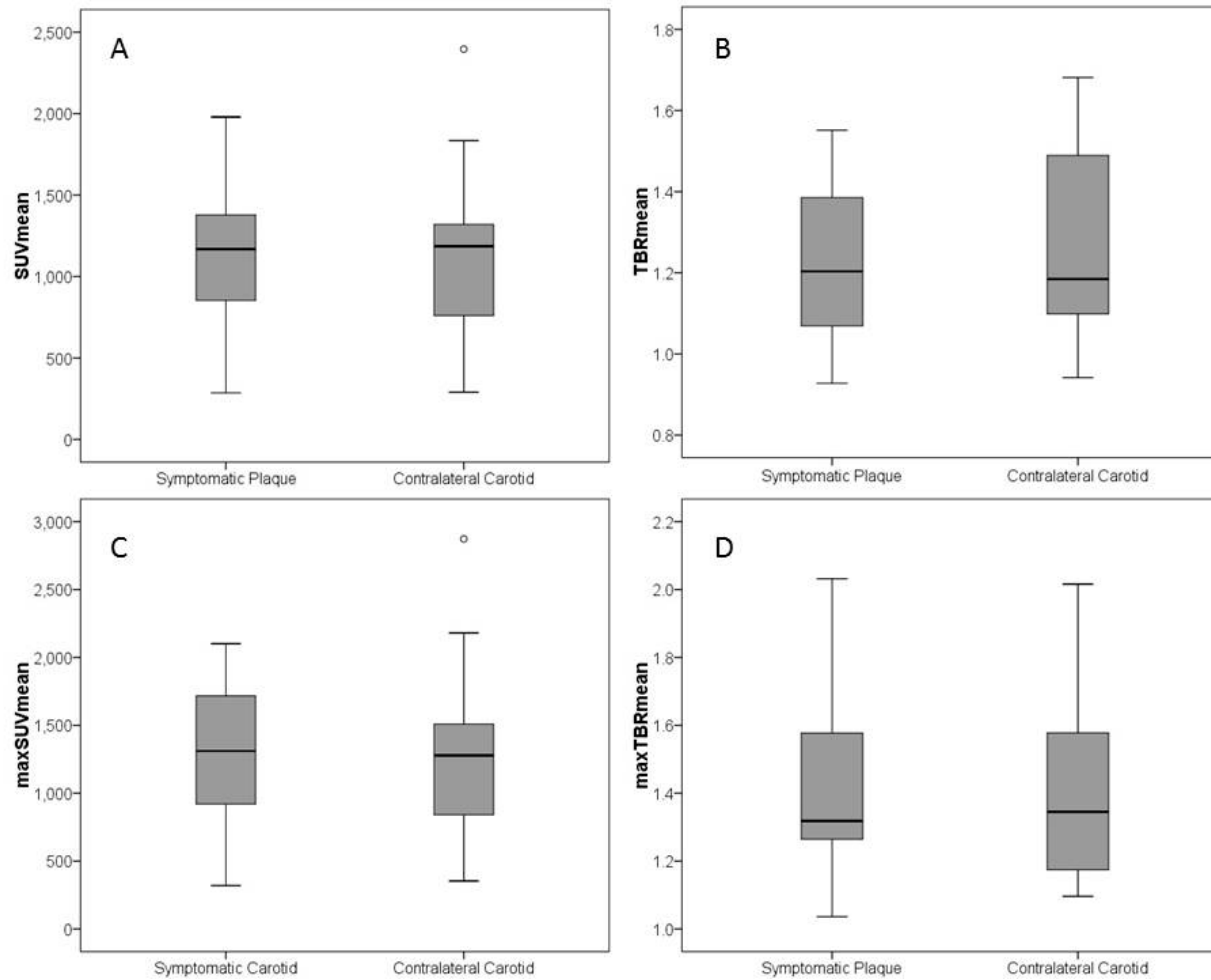
	% Plaque Volume		Volume Plaque Method				Most intense pixel/ROI method			
			SUV max	SUV mean	TBR max	TBR mean	maxSUV max	maxSUVmean	maxTBR max	maxTBR mean
Lipid	32.3+/-10.3	<i>r</i> -value	-0.49	-0.49	-0.08	0.02	-0.37	-0.43	0.03	0.10
		<i>p</i> -value	0.06	0.06	0.78	0.95	0.17	0.11	0.92	0.72
Fibrous	42.5+/-10.6	<i>r</i> -value	-0.12	-0.08	0.05	0.43	-0.04	-0.04	0.01	0.44
		<i>p</i> -value	0.68	0.79	0.85	0.11	0.89	0.90	0.96	0.10
Calcification	25.2+/-14.7	<i>r</i> -value	0.28	0.24	0.00	-0.34	0.18	0.19	-0.03	-0.36
		<i>p</i> -value	0.31	0.39	0.99	0.22	0.52	0.49	0.91	0.18

Supplemental Table 4. Relationship between CD68 immunohistochemistry with Ga68DOTATATE uptake parameters.

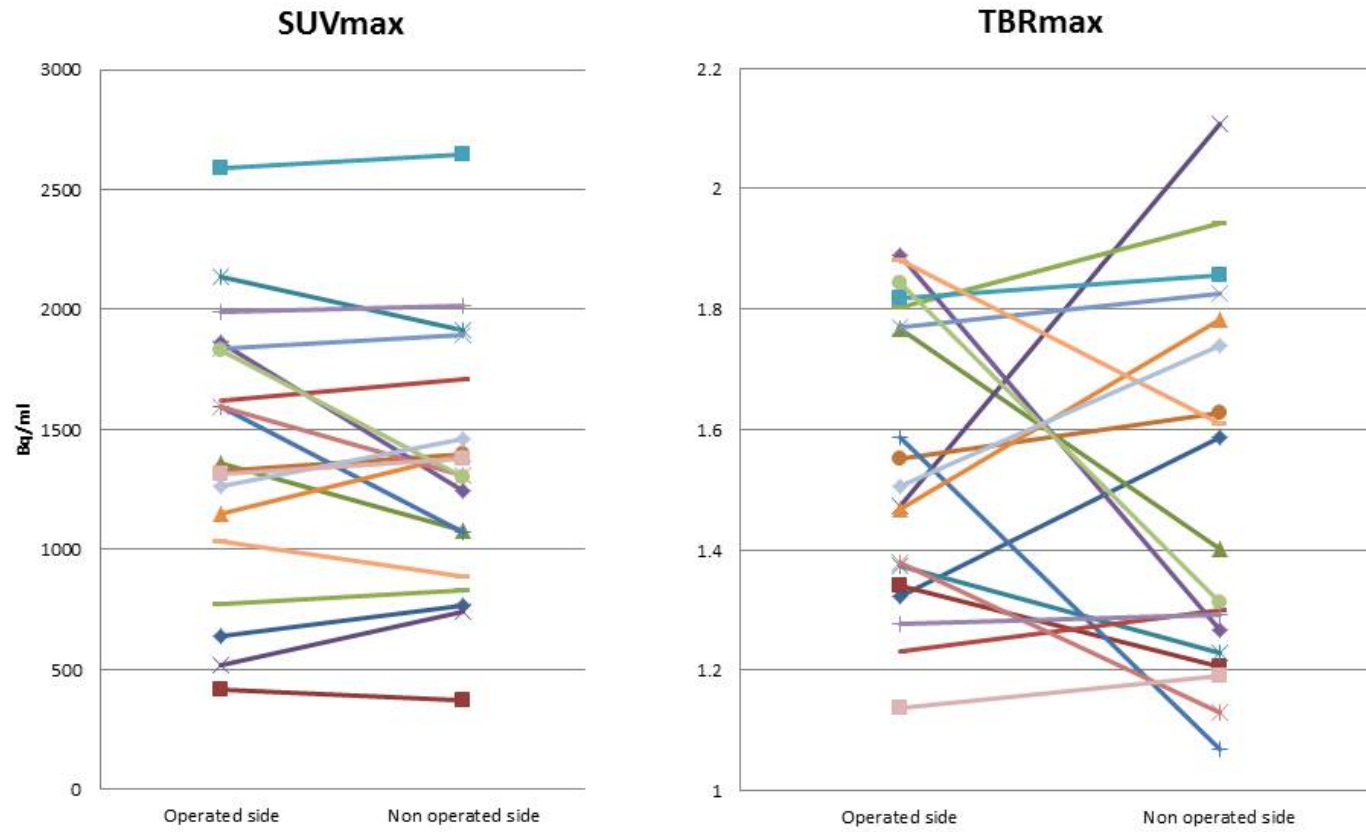
	Volume Plaque Method				Most intense pixel/ROI method			
	SUV max	SUV mean	TBR max	TBR mean	maxSUV max	maxSUV mean	maxTBR max	maxTBR mean
<i>p</i> -value	0.74	0.81	0.9	0.83	0.42	0.68	0.33	0.54



Supplemental Figure 1. Further box plots showing comparison of further PET derived parameters between the symptomatic plaque and contralateral side. A,B: SUVmean and TBRmean from the volume plaque method; C,D: maxSUVmean and maxTBRmean from the most intense pixel/ROI method. (see main text).



Supplemental Figure 2. Example plot of 2 parameters showing individual patient data. (Plots for other parameters not shown).





The Journal of  
NUCLEAR MEDICINE

## PETCT Imaging of Unstable Carotid Plaque with Ga-68 labelled Somatostatin Receptor Ligand

Ming Young Simon Wan, Raymond Endozo, Sofia Michopoulou, Robert Shortman, Manuel Rodriguez-Justo, Leon Menezes, Syed Yusuf, Toby Richards, Damian Wild, Beatrice Waser, Jean Claude Reubi and Ashley Groves

*J Nucl Med.*

Published online: December 8, 2016.

Doi: 10.2967/jnumed.116.181438

---

This article and updated information are available at:  
<http://jnm.snmjournals.org/content/early/2016/12/07/jnumed.116.181438>

---

Information about reproducing figures, tables, or other portions of this article can be found online at:  
<http://jnm.snmjournals.org/site/misc/permission.xhtml>

Information about subscriptions to JNM can be found at:  
<http://jnm.snmjournals.org/site/subscriptions/online.xhtml>

---

*JNM* ahead of print articles have been peer reviewed and accepted for publication in *JNM*. They have not been copyedited, nor have they appeared in a print or online issue of the journal. Once the accepted manuscripts appear in the *JNM* ahead of print area, they will be prepared for print and online publication, which includes copyediting, typesetting, proofreading, and author review. This process may lead to differences between the accepted version of the manuscript and the final, published version.

---

*The Journal of Nuclear Medicine* is published monthly.  
SNMMI | Society of Nuclear Medicine and Molecular Imaging  
1850 Samuel Morse Drive, Reston, VA 20190.  
(Print ISSN: 0161-5505, Online ISSN: 2159-662X)

© Copyright 2016 SNMMI; all rights reserved.

The logo for the Society of Nuclear Medicine and Molecular Imaging (SNMMI) consists of the letters 'S', 'N', 'M', and 'I' arranged in a 2x2 grid. Each letter is white and set within a red square. To the right of this grid, the full name of the society is written in a sans-serif font: 'SOCIETY OF NUCLEAR MEDICINE AND MOLECULAR IMAGING'.

SOCIETY OF  
NUCLEAR MEDICINE  
AND MOLECULAR IMAGING